Polymer Chemistry

PAPER

View Article Online
View Journal | View Issue

Cite this: *Polym. Chem.*, 2016, **7**, 6529

Hyaluronan-coated polybenzofulvene brushes as biomimetic materials†

Andrea Cappelli,*[a] Marco Paolino,[a] Giorgio Grisci,[a] Vincenzo Razzano,[a] Germano Giuliani,[a] Alessandro Donati,[a] Claudia Bonechi,[a] Raniero Mendichi,[b] Salvatore Battiato,[c] Filippo Samperi,[c] Cinzia Scialabba,[d] Gaetano Giammona,[d] Francesco Makovec[e] and Mariano Licciardi[d,f]

Received 19th September 2016,
Accepted 5th October 2016

DOI: 10.1039/c6py01644h

www.rsc.org/polymers

Hyaluronic acid (**HA**) forms pericellular coats in many cell types that are involved in the early stages of cell adhesion by interacting with the CD44 receptor. Based on the largely recognized overexpression of the CD44 receptor in tumor tissues, a polybenzofulvene molecular brush has been enveloped into hyaluronan shells to obtain a tri-component polymer brush (**TCPB**) composed of intrinsically fluorescent backbones bearing nona(ethylene glycol) arms terminated with low molecular weight **HA** macromolecules. The nanoaggregates obtained in **TCPB** water dispersions were characterized on the basis of dimensions, zeta potential, and *in vitro* cell toxicity. This biomimetic multifunctional material bearing **HA** on the surface of its cylindrical brush architecture showed promising prerequisites for the preparation of nanostructured drug delivery systems.

Introduction

Hyaluronic acid (**HA**), also called hyaluronan, is a glycosaminoglycan involved in many important physiological functions in the human body. For example, **HA** has been proposed to form a continuous and relatively thick layer covering the surface of many cells in suspension. Thus, the pericellular **HA** coat has been proposed to play a pivotal role in the early stages of cell adhesion[1] by interacting with the CD44 receptor.[2,3] This receptor is an ubiquitous protein composed of 177 amino acid residues, which forms four domains and among them the extracellular one is called Hyaluronan Binding Domain (HBD) and has been reported to be overexpressed in several tumor tissues.[4]

A large number of different Drug Delivery Systems (DDS) have been developed in order to obtain a modified release of the pharmaceutically active ingredient (API) capable of maintaining the optimal blood level trends.[5,6] Most of these non-conventional dosage forms are based on polymeric materials able to interact with API by means of non-covalent (drug–polymer complexes)[7,8] or covalent attachments to the polymeric backbone (drug–polymer conjugates),[9] and are designed to deliver the API on the basis of their technological features rather than the API chemical and physical ones as it occurs in conventional pharmaceutical forms.[5,6]

Benzofulvene derivatives were shown to polymerize in the apparent absence of catalysts or initiators by a simple removal of solvents to give polybenzofulvene derivatives, which are characterized by intriguing features including susceptibility to molecular manipulation, tunable solubility in different solvents and aggregation behavior in water, and propensity to generate nanostructured aggregates.[10–20] In studying this interesting polymer family, we explored the insertion of oligo(ethylene glycol) (OEG) side chains to obtain the polybenzofulvene molecular brushes (PBFMBs) reported in Fig. 1. These studies suggested that click chemistry reactions such as the copper(I)-catalyzed alkyne–azide 1,3-dipolar cycloaddition (CuAAC) could be used to introduce a large variety of side chains into the polybenzofulvene backbone to design PBFMBs tailored for specific applications.[21] Furthermore, the ability of PBFMBs to complex bioactive mole-

[a]*Dipartimento di Biotecnologie, Chimica e Farmacia and European Research Centre for Drug Discovery and Development, Università degli Studi di Siena, Via A. Moro, 53100 Siena, Italy. E-mail: andrea.cappelli@unisi.it; Tel: +39 0577 234320*
[b]*Istituto per lo Studio delle Macromolecole (CNR), Via E. Bassini 15, 20133 Milano, Italy*
[c]*Istituto per i Polimeri, Compositi e Biomateriali (IPCB) U.O.S. di Catania, CNR, Via Gaifami 18, 95126 Catania, Italy*
[d]*Dipartimento di Scienze e Tecnologie Biologiche, Chimiche e Farmaceutiche (STEBICEF), Università degli Studi di Palermo, Via Archirafi 32, 90123 Palermo, Italy*
[e]*Rottapharm Biotech, Via Valosa di Sopra 9, 20900 Monza, Italy*
[f]*Mediterranean Center for Human Health Advanced Biotechnologies (CHAB), University of Palermo, Italy*

† Electronic supplementary information (ESI) available: Synthetic procedures for the preparation of imidazolide intermediate **7**; ^{1}H NMR spectra of the newly-synthesized poly-6-ANEGA-CMO-**BF3k-GT** and poly-6-ANEGA-CMO-**BF3k-GO** compared with that of macromonomer 6-ANEGA-CMO-**BF3k**; the ^{1}H NMR spectrum of **HA-FA-Pg** compared with that of starting low weight **HA**; the MALDI-TOF mass spectrum (negative-ion mode) of hyaluronan synthon **HA-FA-Pg**; absorption and emission spectra of the **TCPB** material. See DOI: 10.1039/c6py01644h

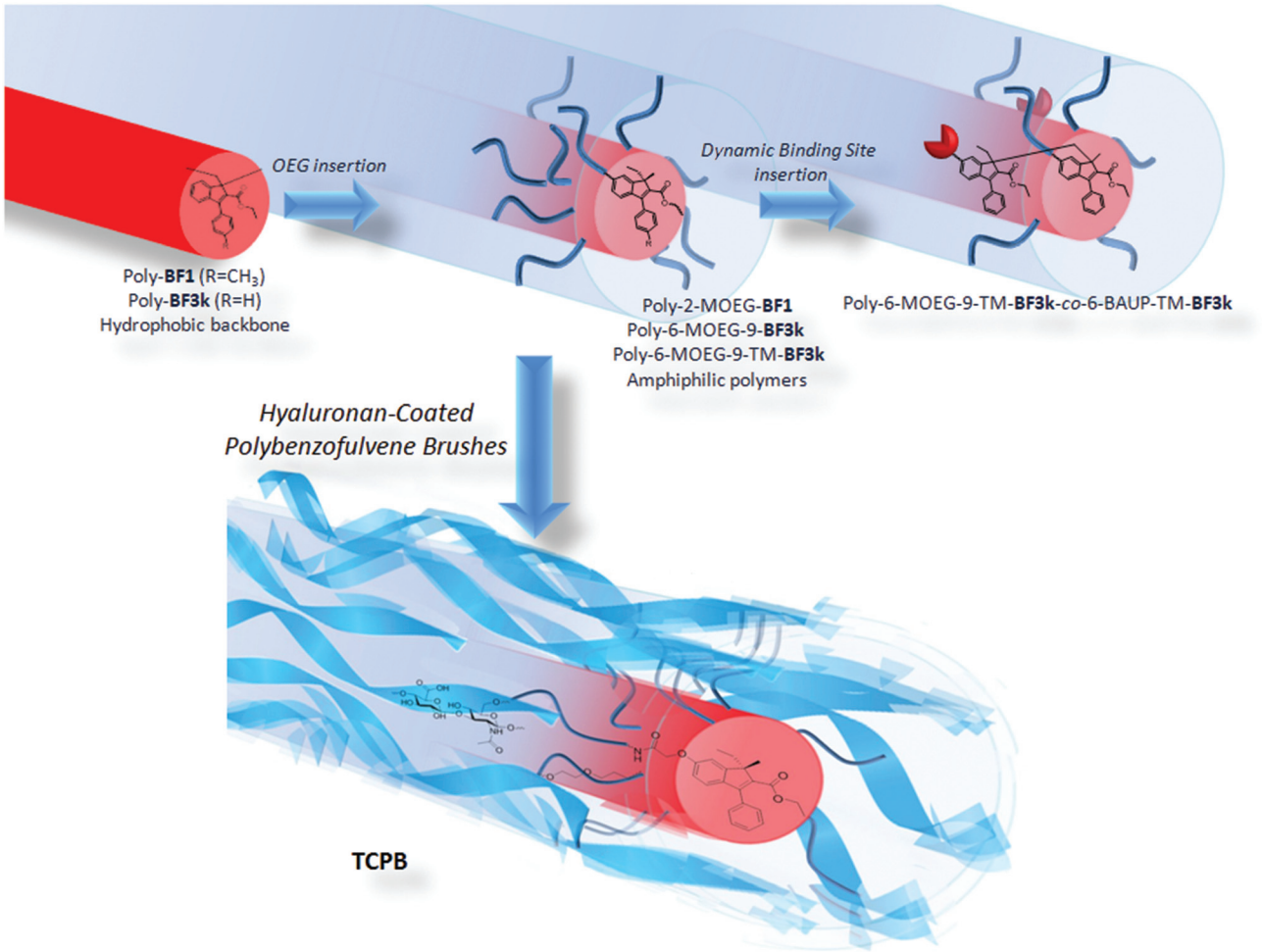

Fig. 1 Development of polybenzofulvene molecular brushes.

cules, such as immunoglobulin G (IgG)[22] or the anticancer peptide leuprolide,[23] was investigated in a strong physical hydrogel obtained with poly-2-MOEG-9-**BF1** or in the nanoaggregates obtained with poly-6-MOEG-9-**BF3k**, respectively. In these systems, the protein–polymer interaction was assumed to occur by non-specific interactions with the hydrogel particles. Finally, PBFMBs bearing synthetic dynamic receptors have been previously used to deliver doxorubicin (**DOXO**) to cancer cells.[21]

In the present paper, a tri-component polymer brush (**TCPB**) was designed by functionalizing the polybenzofulvene backbone with nona(ethylene glycol) (NEG) arms terminated with low molecular weight hyaluronic acid (**HA**) macromolecules (Fig. 1). This work was aimed at developing new advanced functional materials capable of forming biocompatible biomimetic aggregates for biomedical applications.

Experimental section

Synthesis

Melting points were determined in open capillaries in a Gallenkamp apparatus and are uncorrected. Merck silica gel 60 (230–400 mesh) was used for column chromatography. Merck TLC aluminum sheets and silica gel 60 F_{254} were used for TLC. NMR spectra were recorded with a Bruker DRX-400 AVANCE or a Bruker DRX-500 AVANCE spectrometer in the indicated solvents (TMS as internal standard): the values of the chemical shifts are expressed in ppm and the coupling constants (J) in Hz. An Agilent 1100 LC/MSD operating with an electrospray source was used in mass spectrometry experiments.

Ethyl 6-[2-(*tert*-butoxy)-2-oxoethoxy]-1-oxo-3-phenyl-1*H*-indene-2-carboxylate (2). A mixture of indenone **1**[19] (0.28 g, 0.95 mmol), K_2CO_3 (0.39 g, 2.82 mmol), and NaI (0.21 g, 1.40 mmol) in DMF (15 mL) was stirred at room temperature for 10 min, and then *tert*-butyl 2-bromoacetate (0.17 mL, 1.14 mmol) was added. After stirring at room temperature for 18 h, the reaction mixture was treated with a saturated solution of NH_4Cl and extracted with ethyl acetate. The organic layer was dried over Na_2SO_4 and concentrated under reduced pressure. The residue was purified by flash chromatography with petroleum ether–ethyl acetate (7 : 3) as the eluent to afford compound **2** as a red solid (0.37 g, yield 95%, mp 121–122 °C). ^{1}H NMR (400 MHz, $CDCl_3$): 1.14 (t, J = 7.1, 3H),

1.48 (s, 9H), 4.17 (q, J = 7.1, 2H), 4.56 (s, 2H), 6.85 (dd, J = 8.1, 2.4, 1H), 7.08 (d, J = 8.1, 1H), 7.14 (d, J = 2.4, 1H), 7.49 (s, 5H). MS (ESI): m/z 431 ($M + Na^+$).

2-[[2-(Ethoxycarbonyl)-1-oxo-3-phenyl-1*H*-inden-6-yl]oxy]acetic acid (3). A mixture of compound **2** (0.39 g, 0.955 mmol) in formic acid (15 mL) was stirred at room temperature for 1 h. The reaction mixture was then concentrated under reduced pressure and the residue was washed with diethyl ether to afford compound **3** as an orange solid (0.32 g, yield 95%, mp 194–195 °C). ^{1}H NMR (400 MHz, DMSO-d_6): 1.04 (t, J = 7.0, 3H), 4.07 (q, J = 7.0, 2H), 4.81 (s, 2H), 7.00 (d, J = 8.0, 1H), 7.12 (s, 1H), 7.16 (d, J = 8.1, 1H), 7.55 (s, 5H), 13.14 (br s, 1H). MS (ESI): m/z 375 ($M + Na^+$).

Ethyl 6-[(29-azido-2-oxo-6,9,12,15,18,21,24,27-octaoxa-3-azanonacosyl)oxy]-1-oxo-3-phenyl-1*H*-indene-2-carboxylate (4). A solution of **3** (0.14 g, 0.40 mmol) in $SOCl_2$ (5.0 mL) was heated to reflux for 1.5 h and then concentrated under reduced pressure. The residue was dissolved in dry dichloromethane (3.0 mL) and the resulting solution was added to a mixture of *O*-(2-aminoethyl)-*O*′-(2-azidoethyl)heptaethylene glycol (0.27 g, 0.62 mmol) and TEA (0.14 mL) in dry dichloromethane (3.0 mL). The reaction mixture was stirred at room temperature for 1.5 h and then washed in sequence with a saturated solution of $NaHCO_3$ and with brine. The organic layer was dried over Na_2SO_4 and concentrated under reduced pressure. Purification of the residue by flash chromatography with ethyl acetate–methanol (9 : 1) as the eluent gave compound **4** as a red oil (0.22 g, yield 71%). ^{1}H NMR (400 MHz, $CDCl_3$): 1.15 (t, J = 7.1, 3H), 3.37 (t, J = 5.0, 2H), 3.50–3.68 (m, 34H), 4.18 (q, J = 7.0, 2H), 4.53 (s, 2H), 6.86 (dd, J = 8.1, 2.3, 1H), 7.08 (br s, 1H), 7.12 (d, J = 8.1, 1H), 7.22 (d, J = 2.3, 1H), 7.50 (s, 5H). MS (ESI): m/z 795 ($M + Na^+$).

Ethyl 6-[(29-azido-2-oxo-6,9,12,15,18,21,24,27-octaoxa-3-azanonacosyl)oxy]-1-hydroxy-1-methyl-3-phenyl-1*H*-indene-2-carboxylate (5). To a solution of **4** (0.25 g, 0.323 mmol) in dichloromethane (15 mL) was added a 2 M solution of $Al(CH_3)_3$ in toluene (0.65 mL, 1.30 mmol) and the resulting mixture was stirred under a nitrogen atmosphere at room temperature for 30 min and then diluted with ethyl acetate (30 mL). The excess of $Al(CH_3)_3$ was cautiously decomposed by the addition of a 1 N solution of NaOH until the gas evolution ceased. The resulting mixture was washed with water, dried over sodium sulfate, and concentrated under reduced pressure. The residue was purified by flash chromatography with ethyl acetate–methanol (9 : 1) as the eluent to obtain compound **5** as a pale yellow oil (0.22 g, yield 86%). ^{1}H NMR (400 MHz, $CDCl_3$): 1.04 (t, J = 7.1, 3H), 1.76 (s, 3H), 3.33–3.40 (m, 2H), 3.49–3.69 (m, 35H), 4.02–4.19 (m, 2H), 4.54 (s, 2H), 6.82 (d, J = 8.3, 1H), 7.02 (br s, 1H), 7.08 (d, J = 8.3, 1H), 7.16 (s, 1H), 7.32–7.42 (m, 5H). MS (ESI): m/z 811 ($M + Na^+$).

Ethyl 6-[(29-azido-2-oxo-6,9,12,15,18,21,24,27-octaoxa-3-azanonacosyl)oxy]-1-methylene-3-phenyl-1*H*-indene-2-carboxylate (6-ANEGA-CMO-BF3k). A mixture of indenol derivative **5** (10 mg, 0.0127 mmol) in $CDCl_3$ (2.0 mL) with *p*-toluenesulfonic acid monohydrate (PTSA, 2.0 mg, 0.0105 mmol) was heated to reflux for 1 h. The reaction mixture was then cooled at room temperature and washed with a saturated solution of $NaHCO_3$. The organic layer was dried over sodium sulfate to obtain a solution of the corresponding monomer 6-ANEGA-CMO-**BF3k**, which was used in the NMR studies. ^{1}H NMR (500 MHz, $CDCl_3$): 1.04 (t, J = 7.1, 3H), 3.33–3.41 (m, 2H), 3.52–3.68 (m, 34H), 4.11 (q, J = 7.1, 2H), 4.56 (s, 2H), 6.36 (s, 1H), 6.63 (s, 1H), 6.85 (dd, J = 8.4, 2.3, 1H), 7.14 (d, J = 8.4, 1H), 7.16 (br s, 1H), 7.29 (d, J = 2.3, 1H), 7.37–7.46 (s, 5H); see also Fig. S1.† ^{13}C NMR (125 MHz, $CDCl_3$): 13.8, 38.8, 50.7, 60.1, 67.7, 69.7, 70.0, 70.3, 70.5, 70.6, 70.7, 106.9, 114.7, 117.5, 123.4, 124.2, 128.0, 128.3, 128.6, 134.4, 135.7, 139.1, 143.6, 153.0, 158.3, 164.8, 168.0; see also Fig. 3. MS (ESI): m/z 793 ($M + Na^+$).

Poly-[ethyl 6-[(29-azido-2-oxo-6,9,12,15,18,21,24,27-octaoxa-3-azanonacosyl)oxy]-1-methylene-3-phenyl-1*H*-indene-2-carboxylate] (poly-6-ANEGA-CMO-BF3k-GT). A mixture of indenol derivative **5** (0.37 g, 0.469 mmol) in $CDCl_3$ (20 mL) with PTSA (59 mg, 0.31 mmol) was heated under reflux for 1 h. The reaction mixture was then cooled at room temperature and washed with a saturated solution of $NaHCO_3$. The organic layer was dried over sodium sulfate and concentrated under reduced pressure to give a viscous oil, which was dissolved in chloroform (5.0 mL) and newly evaporated (this procedure of dissolution/evaporation was repeated five times). The final residue was dissolved in $CHCl_3$ (3.0 mL) and added dropwise to diethyl ether (10 mL). The resulting dispersion was kept overnight at room temperature. The precipitate was gently separated from the solution and dried under reduced pressure to afford poly-6-ANEGA-CMO-**BF3k-GT** as a brown sticky solid (0.22 g, yield 61%). ^{1}H NMR (500 MHz, $CDCl_3$): see Fig. S1;† ^{13}C NMR (125 MHz, $CDCl_3$): see Fig. 3.

Ethyl 6-(2-*tert*-butoxy-2-oxoethoxy)-1-hydroxy-1-methyl-3-phenyl-1*H*-indene-2-carboxylate (6). To a solution of indenone derivative **2** (0.37 g, 0.906 mmol) in dry dichloromethane (20 mL) cooled at 0–5 °C was added a solution of 2 M $Al(CH_3)_3$ in toluene (0.91 mL, 1.82 mmol) and the resulting mixture was stirred under a nitrogen atmosphere at the same temperature for 5 min. The excess of $Al(CH_3)_3$ was cautiously decomposed by the addition of a 1 N solution of NaOH until the gas evolution ceased. The reaction mixture was partitioned between ethyl acetate and water and the organic layer was dried over sodium sulfate and concentrated under reduced pressure. The residue was purified by flash chromatography with petroleum ether–ethyl acetate–dichloromethane (7 : 2 : 1) as the eluent to afford compound **6** as a pale yellow oil (0.36 g, yield 94%). ^{1}H NMR (400 MHz, $CDCl_3$): 1.04 (t, J = 7.1, 3H), 1.49 (s, 9H), 1.74 (s, 3H), 3.65 (br s, 1H), 4.01–4.21 (m, 2H), 4.57 (s, 2H), 6.81 (dd, J = 8.4, 2.4, 1H), 7.05 (d, J = 8.4, 1H), 7.11 (d, J = 2.4, 1H), 7.30–7.46 (m, 5H). MS (ESI): m/z 447 ($M + Na^+$).

2-[[2-(Ethoxycarbonyl)-1-methylene-3-phenyl-1*H*-inden-6-yl]oxy]acetic acid (6-CMO-BF3k). A mixture of indenol derivative **6** (10 mg, 0.0236 mmol) in $CDCl_3$ (3.0 mL) with PTSA (18 mg, 0.0946 mmol) and sodium sulfate (0.80 g, 5.63 mmol) was heated to reflux for 1 h. The reaction mixture was then cooled at room temperature and washed with 1 N HCl. The organic layer was dried over sodium sulfate to obtain a solution of the

corresponding monomer 6-CMO-**BF3k**, which was used in the NMR studies. ^{1}H NMR (500 MHz, $CDCl_3$): 1.04 (t, J = 7.1, 3H, A), 4.11 (q, J = 7.1, 2H, B), 4.74 (s, 2H, E), 6.34 (s, 1H, Dx), 6.62 (s, 1H, Dy), 6.85 (dd, J = 8.4, 2.4, 1H, 5), 7.14 (d, J = 8.4, 1H, 4), 7.29 (d, J = 2.4, 1H, 7), 7.36–7.47 (s, 5H, Ph). ^{13}C NMR (125 MHz, $CDCl_3$): 13.8 (A), 60.1 (B), 65.1 (E), 106.9 (7), 114.5 (5), 117.5 (D), 123.4 (4), 124.3 (2), 128.0 (3′/5′), 128.3 (4′), 128.6 (2′/6′), 134.4 (1′), 135.9 (3a), 139.1 (7a), 143.5 (1), 153.1 (3), 158.3 (6), 164.9 (C), 171.3 (F); see also Fig. 2. MS (ESI): m/z 373 ($M + Na^+$).

Poly-[2-[[2-(ethoxycarbonyl)-1-methylene-3-phenyl-1*H*-inden-6-yl]oxy]acetic acid] (poly-6-CMO-BF3k). A mixture of indenol derivative **6** (0.28 g, 0.66 mmol) in $CDCl_3$ (80 mL) with PTSA (0.50 g, 2.63 mmol) and sodium sulfate (22 g, 155 mmol) was heated to reflux for 1 h. The reaction mixture was then cooled at room temperature and washed with 1 N HCl. The organic layer was dried over sodium sulfate to obtain a solution of the corresponding monomer 6-CMO-**BF3k**, which was concentrated under reduced pressure to give a glassy solid, which was treated with chloroform (15 mL) and newly evaporated (this procedure of treatment/evaporation was repeated five times). The final residue was purified by washing with dichloromethane and dried under reduced pressure to afford poly-6-CMO-**BF3k** as a pale yellow glassy solid (0.14 g, yield 61%). ^{13}C NMR (125 MHz, DMSO-d_6): see Fig. 2.

Poly-[ethyl 6-[(29-azido-2-oxo-6,9,12,15,18,21,24,27-octaoxa-3-azanonacosyl)oxy]-1-methylene-3-phenyl-1*H*-indene-2-carboxylate] (poly-6-ANEGA-CMO-BF3k-GO). A mixture of poly-6-CMO-**BF3k** (50 mg, 0.143 mmol) in $SOCl_2$ (5.0 mL) was refluxed for 1.5 h and then concentrated under reduced pressure. The residue was dissolved in dry dichloromethane (5.0 mL) and the resulting solution was treated with a solution of *O*-(2-aminoethyl)-*O*′-(2-azidoethyl)heptaethylene glycol (120 mg, 0.274 mmol) and TEA (0.10 mL) in dry dichloromethane (3.0 mL). The reaction mixture was stirred overnight at room temperature and then partitioned between dichloromethane and a saturated $NaHCO_3$ solution. The organic layer was washed with brine, dried over Na_2SO_4 and concentrated under reduced pressure. Purification of the residue by precipitation with diethyl ether (15 mL) from a dichloromethane solution (3.0 mL) gave poly-6-ANEGA-CMO-**BF3k-GO** as a brown sticky solid (64 mg, yield 58%). ^{1}H NMR (500 MHz, $CDCl_3$): see Fig. S1;† ^{13}C NMR (125 MHz, $CDCl_3$): see Fig. 3.

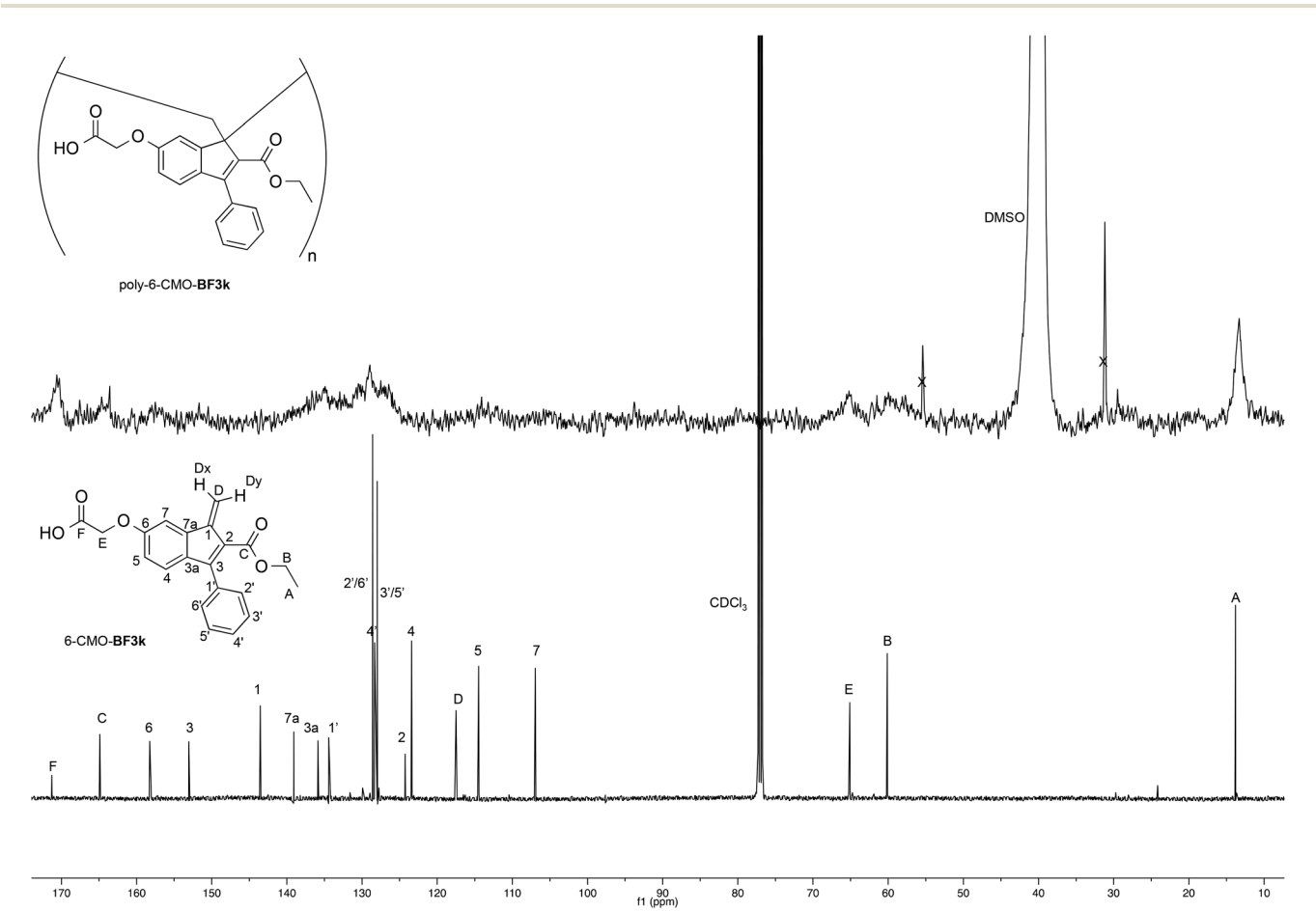

Fig. 2 ^{13}C NMR spectrum (DMSO-d_6) of poly-6-CMO-**BF3k** compared with that of the corresponding monomer 6-CMO-**BF3k**.

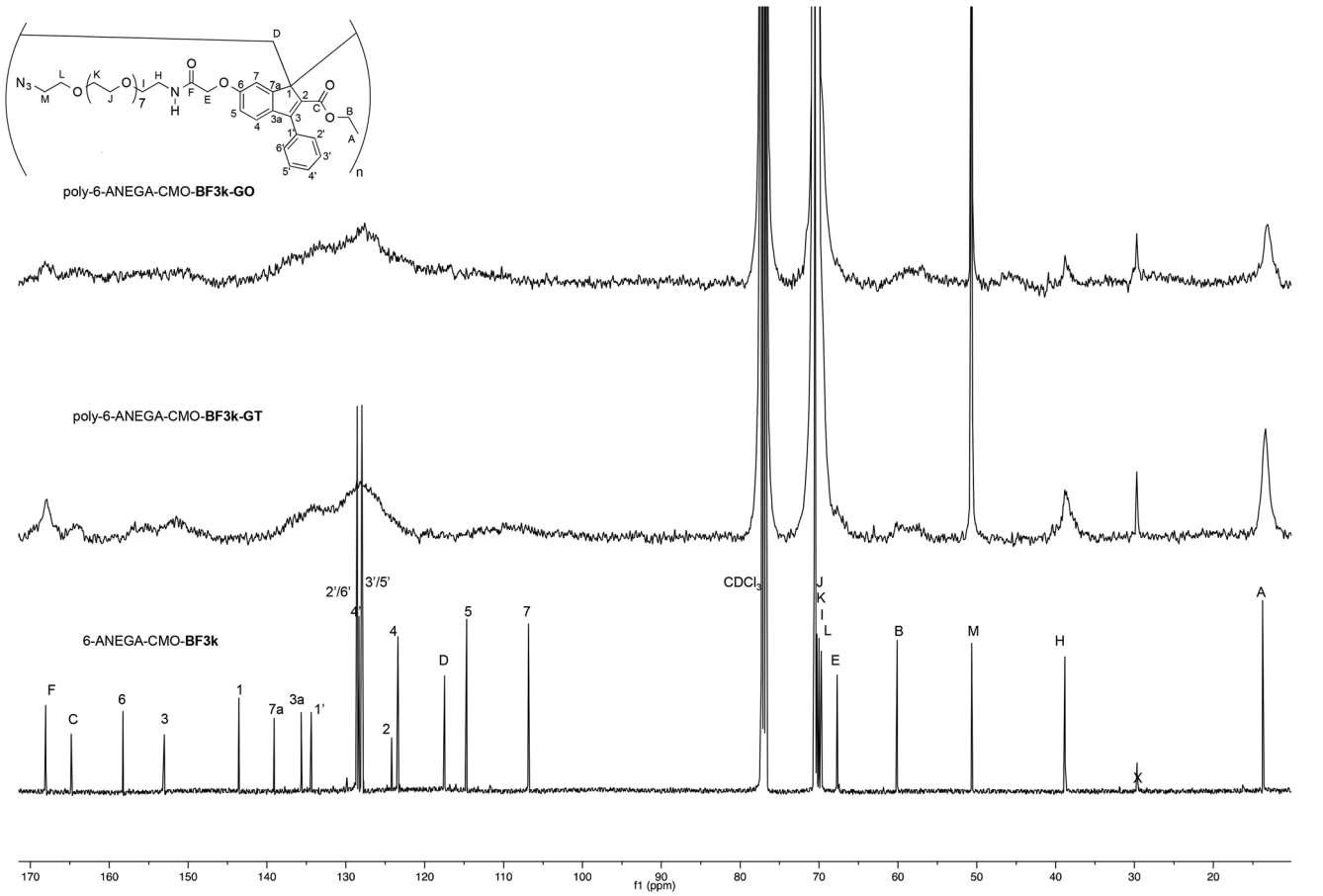

Fig. 3 ^{13}C NMR spectra ($CDCl_3$) of newly-synthesized poly-6-ANEGA-CMO-**BF3k-GT** and poly-6-ANEGA-CMO-**BF3k-GO** compared with that of macromonomer 6-ANEGA-CMO-**BF3k**.

Procedure for the synthesis of the hyaluronan synthon HA-FA-Pg

A mixture of low molecular weight **HA** (1.0 g, 2.64 mmol in monomeric units) in formamide (10 mL) was heated at about 50 °C until complete dissolution was achieved. The resulting solution was then cooled to room temperature and TEA (0.37 mL, 2.66 mmol) and 7 (0.186 g, 0.659 mmol) were sequentially added. The reaction mixture was stirred overnight at room temperature and then diluted with a 5% NaCl solution (5.0 mL). The resulting mixture was stirred at room temperature for 10–15 min. Finally, the polymer was obtained by treatment of the mixture with acetone (40 mL) and purified by washing four times with the same solvent. The final solid was dried under reduced pressure to afford the expected **HA-FA-Pg** graft copolymer as a white solid (1.05 g). ^1H NMR (500 MHz, D_2O): see Fig. S3;† ^{13}C NMR (125 MHz, D_2O): see Fig. 6.

Preparation of the tri-component polybenzofulvene molecular brush TCPB

A round bottom 10 mL flask was charged under an inert atmosphere with *tert*-butanol (2.0 mL), water (2.0 mL), and a solution of $CuSO_4$ pentahydrate (12.5 mg, 0.050 mmol) in 0.50 mL of water. Then, a 1 M solution of sodium ascorbate in water (0.50 mL) was added and 1.0 mL of the resulting mixture was used as the catalyst. A mixture of poly-6-ANEGA-CMO-**BF3k** (50 mg) and **HA-FA-Pg-3F** (50 mg) in 10 mL of *tert*-butanol–water (1 : 1) was treated with the catalyst solution (1.0 mL) and the reaction mixture was stirred overnight at room temperature and then concentrated under reduced pressure. The residue was dissolved in 25 mL of ethanol–water (2 : 1) and QUADRASIL MP (200 mg) was added. After filtration the solution was concentrated under reduced pressure. The residue was dissolved in 5.0 mL of ethanol–water (2 : 1) and the solution was added dropwise into acetone (45 mL). The resulting suspension was decanted overnight to furnish a fine precipitate, which was gently separated from the solution and dried under reduced pressure to obtain **TCPB** as a brown glassy solid (94 mg). ^{13}C NMR (125 MHz, D_2O): see Fig. 7.

SEC-MALS

The molecular characterization was performed by using a multi-angle laser light scattering (MALS) photometer on line to a size exclusion chromatography (SEC) system. The SEC-MALS system consisted of an Alliance 2695 chromatograph from

Waters (USA), a MALS Dawn DSP-F photometer from Wyatt (USA), and a 410 differential refractometer from Waters as a concentration detector. In detail, the experimental conditions were the following: 0.2 M NaCl + DMSO (50/50 w/w), 35 °C of temperature, 0.5 mL min^{-1} of flow rate, and two Polargel (M-L) columns from Polymers Laboratories (UK).

The MALS photometer used a vertically polarized He–Ne laser (λ = 632.8 nm) and simultaneously measured the intensity of the scattered light at 18 angular locations ranging from 14.7° to 151.7°. The calibration constant was calculated using toluene as a standard assuming a Rayleigh factor of 1.406 × 10^{-5} cm^{-1}. The angular normalization was performed by measuring the scattering intensity of a concentrated solution of a pullulan standard showing a narrow MWD (M_p = 12 kg per mole, M_w/M_n < 1.03, R_g = 2.1 nm) assumed to act as an isotropic scatterer. It is known that the on-line MALS detector measures, for each polymeric fraction eluted from the columns, the molecular weight (M) and when the angular dependence of the scattered light is experimentally measurable, also the molecular size generally known as the gyration radius (R_g). The SEC-MALS system is described in detail elsewhere.[24,25]

The differential refractive index increment for the polymers with respect to the mixed solvent was measured off-line by using a Chromatix KMX-16 differential refractometer. The dn/dc value was 0.116 mL g^{-1} for **HA** and 0.122 mL g^{-1} for **HA-FA-Pg**.

MALDI-TOF MS

MALDI TOF MS (matrix assisted laser desorption/ionization time of flight mass spectrometry) mass spectra were recorded using a 4800 Proteomic Analyzer (Applied Biosystems) MALDI-TOF/TOF instrument equipped with a Nd:YAG laser at a wavelength of 355 nm with <500 ps pulse and 200 Hz firing rate, and the acceleration voltage was set at 20 kV. The irradiance was maintained slightly above the threshold, to obtain a mass resolution of about 1000–2000 fwhm; isotopic resolution was observed throughout the entire mass range detected (from m/z 1000 up to m/z 6000). External calibration was performed using an Applied Biosystems calibration mixture consisting of polypeptides with different molecular weight values. Mass accuracy was about 150–200 ppm. All measurements were performed in negative ion mode; approximately 1500 laser shots were accumulated for each mass spectrum. The best spectra were recorded using 2,5-DHB as a matrix (0.1 M in CH_3CN/CH_3OH 1/1 v/v). Polymer samples were solubilized in the CH_3CN/CH_3OH (1 : 1 v/v) solvent mixture with a concentration of about 2 mg mL^{-1}. Samples for MALDI analysis were prepared by the dried-droplet method, in which a mixture of matrix and sample (0.3 μL) was deposited onto the target plate and dried at room temperature under an inert atmosphere (N_2 flow).

Preparation of TCPB nanoparticles

25 mg of **TCPB** were dissolved in 4.0 mL of DMSO and the obtained mixture was sonicated for 30 min and dialyzed for 48 h against double distilled water using Spectra Por Dialysis with a molecular weight cut-off (MWCO) of 25 000 Da. After 48 h, the nanoparticle dispersion was filtered through a 5 μm cellulose membrane filter, frozen by immersion in liquid nitrogen and freeze-dried from water.

Dynamic light scattering (DLS) analysis and ζ potential measurements

The mean diameter, width of distribution (polydispersity index, PDI), and ζ potential of the nanoparticles were measured at 25 °C using a Zetasizer NanoZS instrument fitted with a 532 nm laser at a fixed scattering angle of 173°. The intensity-average hydrodynamic diameter (size in nm) and PDI of **TCPB** nanosystems (0.2 mg mL^{-1}) were measured in double distilled water. The ζ potential (mV) was calculated from the electrophoretic mobility using the Smoluchowski relationship and assuming that $Ka \gg 1$ (where K and a are the Debye–Hückel parameter and particle radius, respectively). Each experiment was performed in triplicate.

Cytotoxicity evaluation

The cytotoxicity was assessed by the tetrazolium salt (MTS) assay on three cell lines; human colon cancer (HCT116), human breast adenocarcinoma (MCF-7), and human bronchial epithelial (16HBE) cell lines (purchased from Istituto Zooprofilattico Sperimentale della Lombardia e dell'Emilia Romagna, Italy) using a commercially available kit (Cell Titer 96 Aqueous One Solution Cell Proliferation assay, Promega). Cells were seeded in 96 well plates at a density of 2.5 × 10^4 cells per well and grown in Dulbecco's Minimum Essential Medium (DMEM) with 10% FBS (foetal bovine serum) and 1% of penicillin/streptomycin (10 000 U mL^{-1} penicillin and 10 mg mL^{-1} streptomycin) at 37 °C in a 5% CO_2 humidified atmosphere. After 24 h of cell growth the medium was replaced with 200 μL of fresh culture medium containing **TCPB** nanoparticles at concentrations corresponding to 20, 40, 80 and 200 μg mL^{-1}. After 24 and 48 h of incubation time, DMEM was replaced with 100 μL of fresh medium and 20 μL of a MTS solution was added to each well. The plates were incubated for an additional 2 h at 37 °C. Then, the absorbance at 490 nm was measured using a microplate reader (Multiskan, Thermo, UK). Pure cell medium was used as a negative control. Results were expressed as percentage reduction of the control cells. All culture experiments were performed in triplicate.

Statistical analysis

A one way analysis of variance (ANOVA) was applied to compare different groups. Data were considered statistically significant with a value of P < 0.05 and differences between different groups were compared using *a posteriori* Bonferroni t-test. All values are expressed as the average of three experiments ± standard deviation.

Results and discussion

Synthesis of the tri-component polybenzofulvene molecular brush (TCPB)

The preparation of the tri-component polybenzofulvene molecular brush **TCPB** was carried out by means of a convergent approach consisting of three different steps: the preparation of the polybenzofulvene backbone bearing nona(ethylene glycol) (NEG) arms terminated with clickable azido groups (Schemes 1 and 2), the functionalization of low molecular weight hyaluronic acid (**HA**) macromolecules with ferulic acid (**FA**) bearing clickable propargyl groups (Scheme 3), and the coupling between the two macromolecular synthons by copper(I)-catalyzed azide–alkyne 1,3-dipolar cycloaddition (CuAAC, Scheme 4).

The polybenzofulvene synthon was firstly synthesized by means of a "grafting through" approach (Scheme 1) in order to obtain a structurally homogeneous cylindrical brush showing the maximum grafting degree (GD, *i.e.* each monomeric unity bears its NEG side chain).

The phenol group of indenone derivative **1** [19] was alkylated with *tert*-butyl 2-bromoacetate in the presence of potassium carbonate as the base and sodium iodide as the catalyst in *N*,*N*-dimethylformamide to afford diester **2**. The *tert*-butyl ester group of **2** was cleaved under acidic conditions to obtain acetic acid derivative **3**, which was activated with thionyl chloride

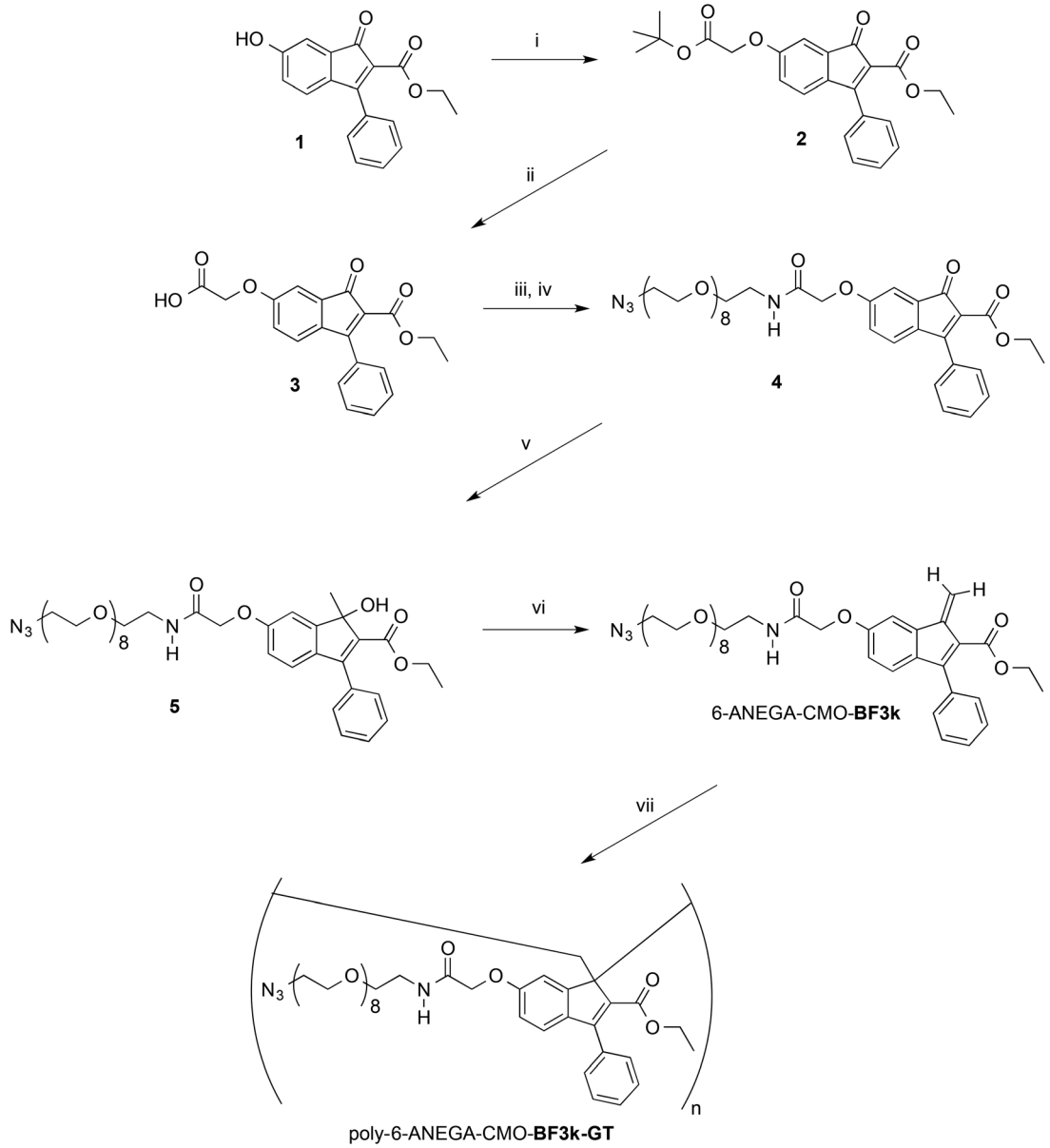

Scheme 1 "Grafting through" approach to the preparation of the polybenzofulvene synthon. Reagents: (i) *tert*-butyl 2-bromoacetate, K_2CO_3, NaI, DMF; (ii) HCOOH; (iii) $SOCl_2$; (iv) $N_3(CH_2CH_2O)_8CH_2CH_2NH_2$, TEA, CH_2Cl_2; (v) $Al(CH_3)_3$, CH_2Cl_2; (vi) PTSA, $CDCl_3$; (vii) solvent elimination.

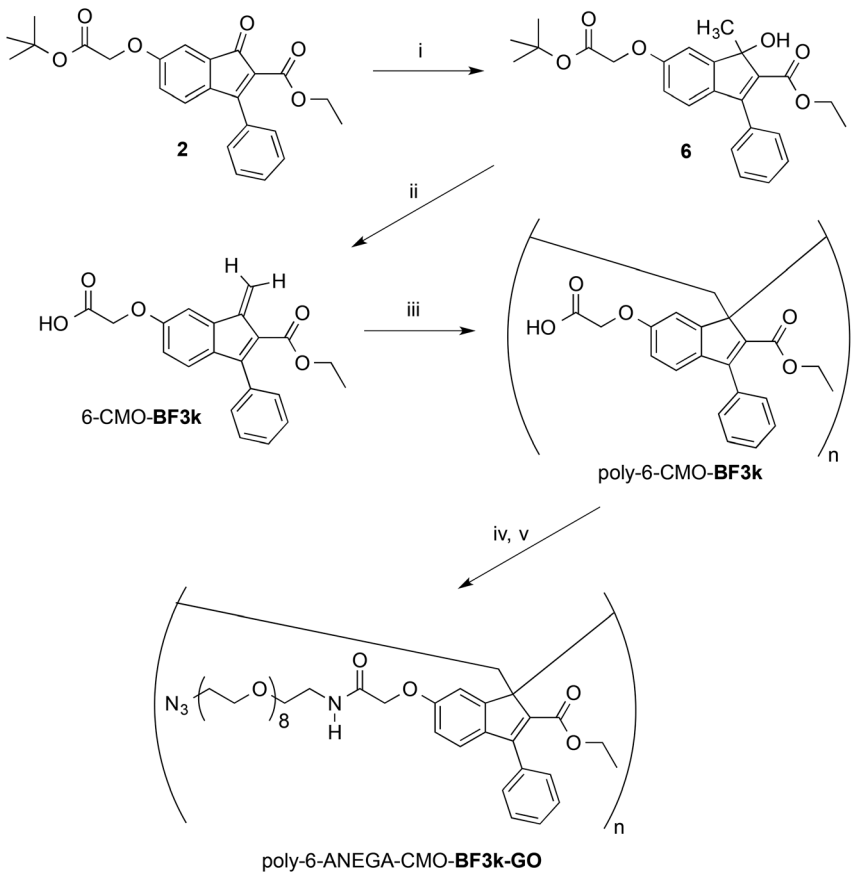

Scheme 2 "Grafting onto" approach to the preparation of the polybenzofulvene synthon. Reagents: (i) $Al(CH_3)_3$, CH_2Cl_2; (ii) PTSA, Na_2SO_4, $CDCl_3$; (iii) solvent elimination; (iv) $SOCl_2$; (v) $N_3(CH_2CH_2O)_8CH_2CH_2NH_2$, TEA, CH_2Cl_2.

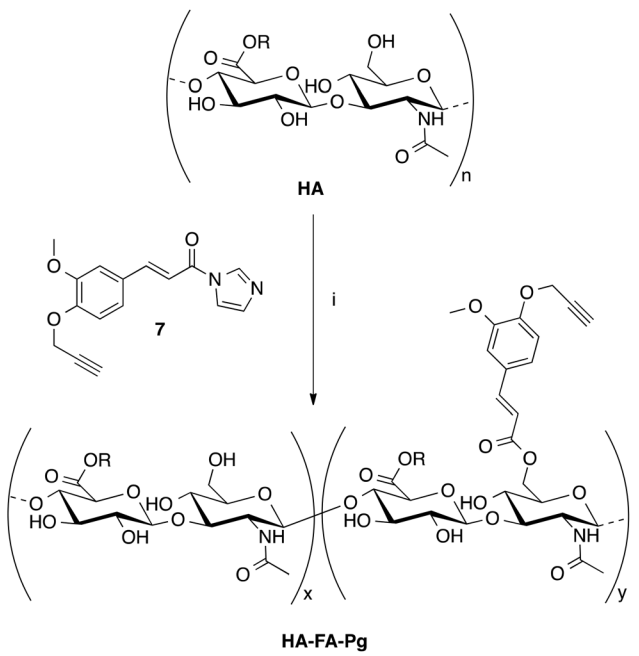

Scheme 3 Preparation of the hyaluronan synthon **HA-FA-Pg**. Reagents: (i) $HCONH_2$, TEA. Substituents: R = H or C_2H_5.

and transformed into acetamide derivative **4** by reaction with alpha-azido-omega-amino nona(ethylene glycol) (azido-NEG-amine) in the presence of TEA as the base. Amide **4** was used in the usual methylation/dehydration procedure to obtain benzofulvene macromonomer 6-ANEGA-CMO-**BF3k**, which was thoroughly characterized by NMR spectroscopy and allowed to polymerize spontaneously by solvent removal to afford the corresponding polymer poly-6-ANEGA-CMO-**BF3k-GT**. Then, the polybenzofulvene synthon was prepared by means of a "grafting onto" approach (poly-6-ANEGA-CMO-**BF3k-GO**, Scheme 2) and compared with poly-6-ANEGA-CMO-**BF3k-GT**.

In particular, diester **2** was used as the starting material in the classical multistep sequence used in the preparation of polybenzofulvene derivatives (*i.e.* the methylation/dehydration procedure followed by the spontaneous polymerization) in order to obtain poly-6-CMO-**BF3k**. The optimization of the dehydration reaction leading to acid monomer 6-CMO-**BF3k** required hard work, and after several attempts, this compound was isolated in sufficient purity to be used in a careful structural characterization by NMR spectroscopy and allowed to polymerize spontaneously by solvent removal to afford the corresponding polymer poly-6-CMO-**BF3k**. After confirming its structure by ^{13}C NMR spectroscopy (Fig. 2), the polymer was

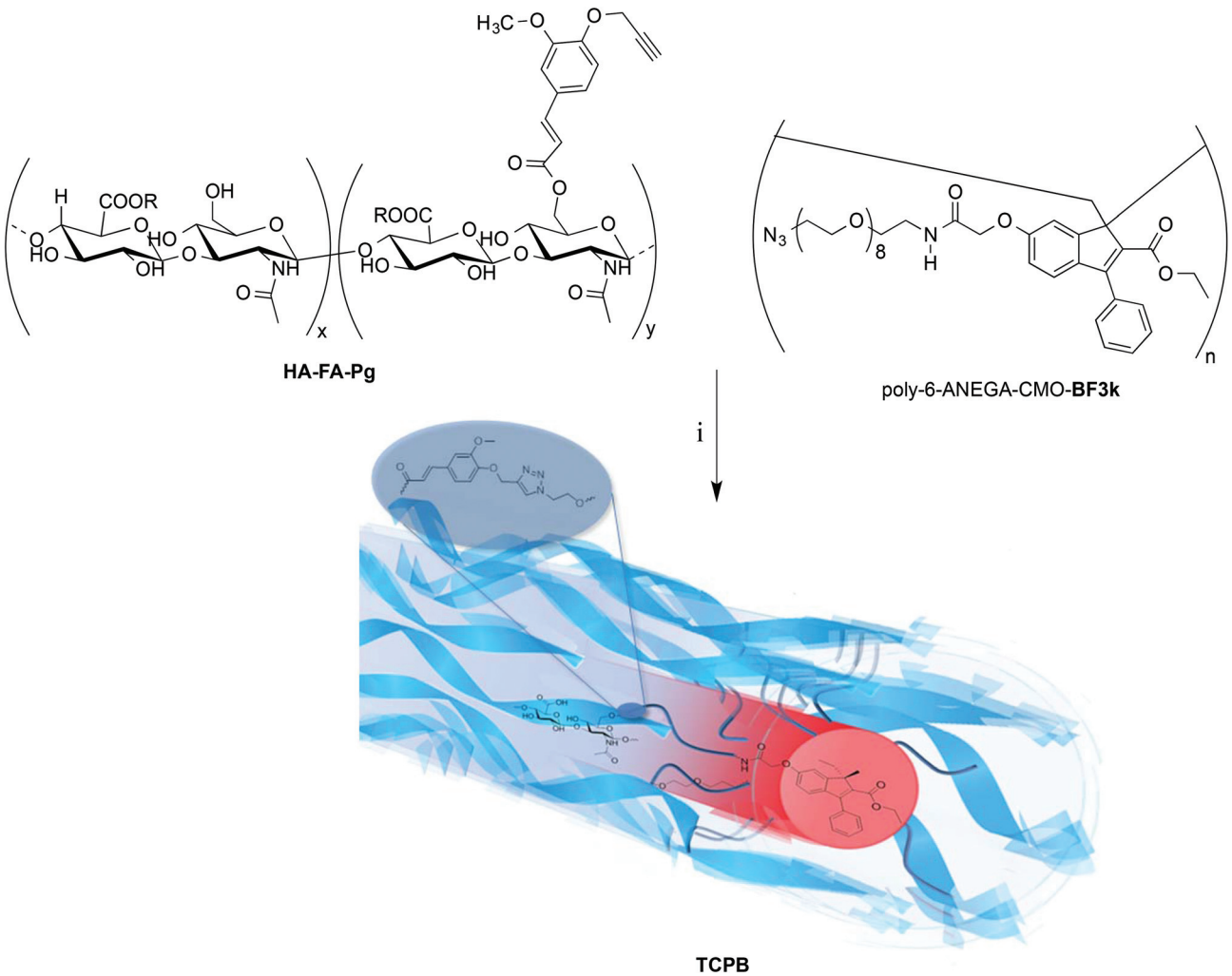

Scheme 4 Click chemistry functionalization of poly-6-ANEGA-CMO-**BF3k** with hyaluronan synthon **HA-FA-Pg**. Reagents: (i) $CuSO_4$, sodium ascorbate, *tert*-BuOH, H_2O. Substituents: R = H or C_2H_5.

solubilized in refluxing thionyl chloride and, after the removal of excess thionyl chloride, it was reacted with azido-NEG-amine in the presence of TEA as the base to give poly-6-ANEGA-CMO-**BF3k-GO**.

Both polybenzofulvene brushes poly-6-ANEGA-CMO-**BF3k-GT** and poly-6-ANEGA-CMO-**BF3k-GO** were obtained as light brown sticky solids showing a good solubility in chloroform, but they were only partially soluble in water as shown by the presence of the appropriate signals in their ^{1}H NMR spectra performed with water dispersions (data not shown). The solubility of polybenzofulvene brushes poly-6-ANEGA-CMO-**BF3k-GT** and poly-6-ANEGA-CMO-**BF3k-GO** in chloroform allowed the characterization of their NMR spectra to be easily recorded and compared with those of the corresponding macromonomer 6-ANEGA-CMO-**BF3k**. In particular, the ^{1}H and ^{13}C NMR spectra of the latter were carefully assigned by means of 2D correlation experiments and used as references in order to evaluate the retention of the original vinyl (1,2) polymerization mechanism. However, the ^{1}H NMR spectra of both poly-6-ANEGA-CMO-**BF3k-GT** and poly-6-ANEGA-CMO-**BF3k-GO** (Fig. S1, see the ESI†) are dominated by the very intense signals of the NEG side chains that appeared quite sharp with respect to the ones of the polybenzofulvene backbone that were very broad. This result is consistent with the higher mobility shown by the NEG side chain with respect to the slow dynamics of the polymer main chain, but the comparison failed in providing further structural information.

On the other hand, the corresponding ^{13}C NMR spectra of the polybenzofulvene brushes poly-6-ANEGA-CMO-**BF3k-GT** and poly-6-ANEGA-CMO-**BF3k-GO** were sufficiently resolved to be compared with the corresponding spectrum of the macromonomer 6-ANEGA-CMO-**BF3k** (Fig. 3). Thus, the enchainment of the polybenzofulvene derivatives was confirmed on the basis of the chemical shift values of the previously defined diagnostic peaks.[11,13,14,20] These include: the peak of the aliphatic quaternary carbon (C-1) of the 1,2-repeating indene unit (at around 57 ppm), the peak of the carbon (C–D) of the methylene bridge linking the monomeric units along the poly-

benzofulvene backbone (at around 45–48 ppm), and the peaks of the indene carbon atoms (C-1′ and C-3), which may be affected by the competing 1,4-polymerization.

Unfortunately, the apparent broadness of the signals attributed to the polybenzofulvene backbone was superior to the one previously observed in some other polymers belonging to the same family, but it was absolutely consistent with the broadening effect generated by the introduction of the NEG side chain in polybenzofulvene derivatives. We assume that the architecture of the PBFMB led to self-aggregating features, which limit the presence of isolated macromolecules under the conditions used in NMR studies (*i.e.* polymer concentration in the order of 20 mg mL^{-1}) and drastically decrease the resolution of carbon atoms belonging to the polymeric backbone. Even taking into account these limitations, the presence of the above-defined diagnostic peaks suggested the 1,2-enchainment as the fundamental structural motif also for the backbones of these PBFMBs.

The comparison of the spectroscopic features of poly-6-ANEGA-CMO-**BF3k-GO** with those of poly-6-ANEGA-CMO-**BF3k-GT** confirmed the viability of the "grafting onto" approach in the preparation of this polybenzofulvene cylindrical brush and paves the way to the synthesis of molecular brushes tailored for specific applications. The better resolution observed in the ^{13}C NMR spectra of poly-6-ANEGA-CMO-**BF3k-GT**, the polymer obtained by the grafting through approach, with respect to the corresponding one obtained by the grafting onto approach, could be related to possible differences in molecular weight and aggregation liability.

The hyaluronan synthon was prepared by functionalization of hyaluronic acid macromolecule with ferulic acid bearing a clickable propargyl group as shown in Scheme 3.

In particular, the reaction of imidazolide 7 (see the ESI† for the preparation) with low molecular weight hyaluronic acid in the presence of TEA as the base in formamide as the solvent gave the expected graft copolymer **HA-FA-Pg**, which was obtained as a white solid by precipitation with acetone. The graft copolymer showed good water solubility and was characterized by means of a multi-angle laser light scattering (MALS) detector on-line to a size exclusion chromatography (SEC) apparatus, by MALDI-TOF mass spectrometry and NMR spectroscopy in order to assess the molecular weight distribution (MWD) features and the grafting degree (GD, *i.e.* the number of the clickable propargyl-**FA** moieties in each low molecular weight **HA** macromolecule).

The SEC-MALS results summarized in Table 1 suggest that the mild conditions used in the grafting reaction produced only negligible changes in the apparent MWD of the graft copolymer.

Both unfunctionalized **HA** and functionalized **HA-FA-Pg** samples were characterized by MALDI-TOF MS in negative-ion mode, using DHB as the matrix. The mass spectrum of neat oligosaccharide **HA** (Fig. 4) shows, in the mass range *m*/*z* 2500–10 000 Da, a series of clusters corresponding to the even-numbered **HA** oligosaccharides (7- to 23-mers, species A_n).

The first peak of each cluster corresponds to the $[M - H]^-$ ions of the **HA** oligosaccharides corresponding to the species A_n (*i.e.* peak at *m*/*z* 4347 in the inset of Fig. 4). Within each cluster, peaks differ by 28 Da matching the mass of ethyl ester groups as can be observed in the inset reported in Fig. 4. Indeed, the ions at *m*/*z* 4375, 4403, 4431, 4459 and 4487 correspond to the esterified oligosaccharide chains bearing one, two, three, four, and five ethyl ester groups along the chains, respectively (species A'_n, where the apex indicates the number of ethyl esters). Considering the relative intensity of the peak corresponding to unesterified chains ($[M - H]^-$ ions) and those of different esterified oligosaccharides we have estimated that of about 32–35% mol of the initial **HA** sample present ethyl esterified carboxyl groups. Complex mass spectra were recorded in the case of the hyaluronan graft copolymer **HA-FA-Pg** (Fig. S2, see the ESI†), which shows a series of cluster of peaks in the mass range *m*/*z* 3500–10 000. An enlarged section of this mass spectrum is reported in Fig. 5 together with the structural assignment.

The spectrum shows that the most intense peaks belong to the expected graft copolymer chains (species $A_{x,y}$). In particular, it suggests that most of the copolymer chains present 4 or 5 clickable propargyl groups along the backbone. The corresponding copolymer chains containing ethyl ester groups (species $A'_{x,y}$) were also revealed in accord to the mass spectrum of the initial **HA** sample (Fig. 4). The mass spectrum also reveals the presence of unfunctionalized oligosaccharides (species A_n and A'_n, *i.e.* peaks 4347, 4375, 4403 and 4431 in Fig. 5). Thus, the MALDI mass spectra confirmed the formation of the reactive functionalized oligosaccharides.

A further confirmation was obtained also by the NMR studies. In fact, when the ^1H NMR spectrum of **HA-FA-Pg** was compared with that of the starting low weight **HA** (Fig. S3, see the ESI†), the presence of a well recognized signal pattern in the aromatic region suggested the occurrence of the designed functionalization.

As expected, the comparison of the corresponding ^{13}C NMR spectra (Fig. 6) was again more informative because of the more resolved spectral lines. The assignment of the ^{13}C NMR spectrum of the starting low molecular **HA** was performed by integrating the results of the NMR studies performed in our laboratories with those reported in the literature.[26] It is noteworthy that the ^{13}C NMR spectrum of the hyaluronan synthon **HA-FA-Pg** showed a well resolved set of signals that were assigned to the ferulate moiety on the basis of the results of the NMR studies performed with methyl ferulate intermediate

Table 1 Comparison of the macromolecular features of graft copolymer **HA-FA-Pg** with those of starting low molecular weight **HA**

Polymer	M_p (kg mol^{-1})	M_w [a] (kg mol^{-1})	M_w/M_n [b]
HA-FA-Pg	6.8	6.5	1.45
HA	8.5	8.7	1.53

[a] M_w: weight-average molecular weight. [b] Dispersity where M_n denotes the numeric-average molecular weight.

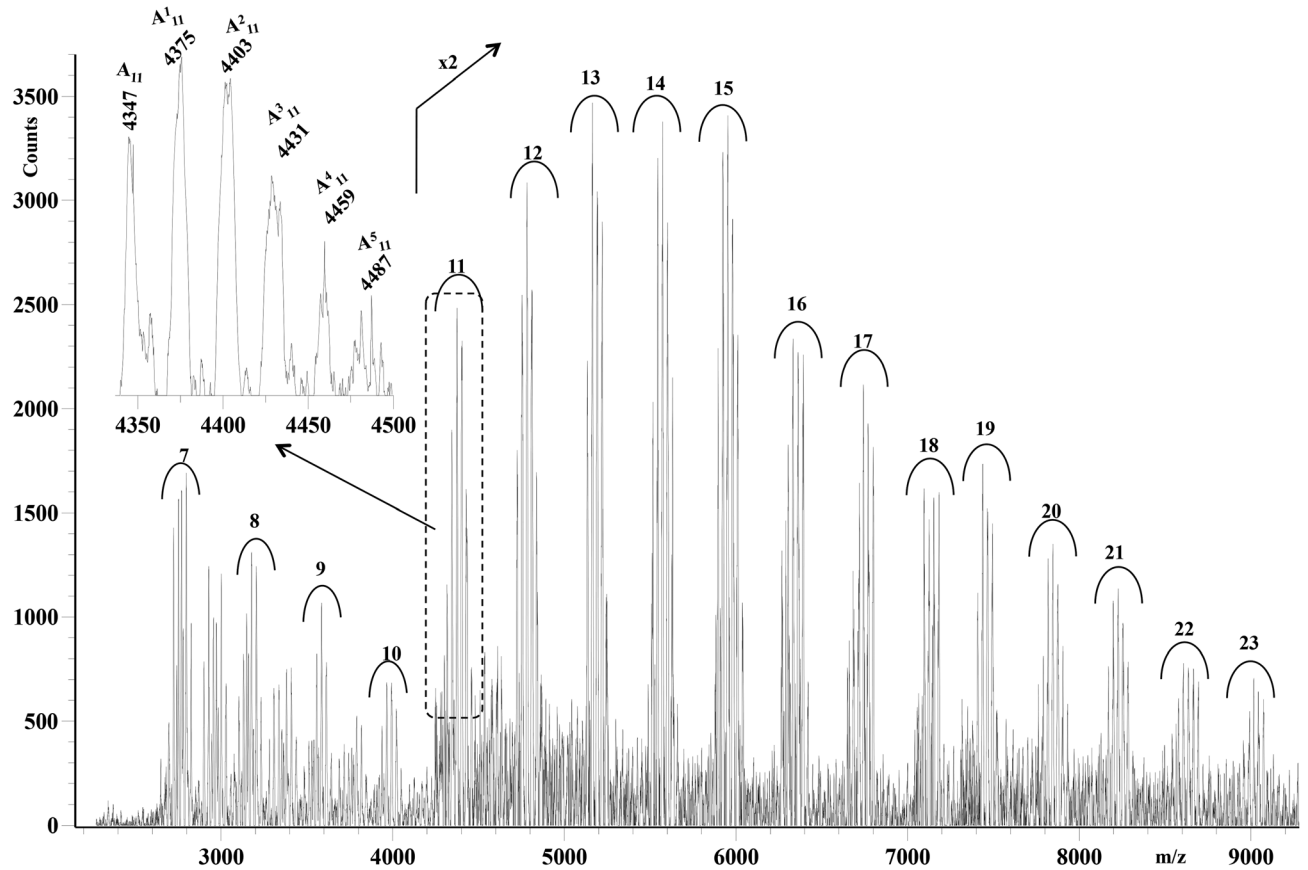

Fig. 4 MALDI-TOF mass spectrum (negative-ion mode) of starting low molecular weight HA.

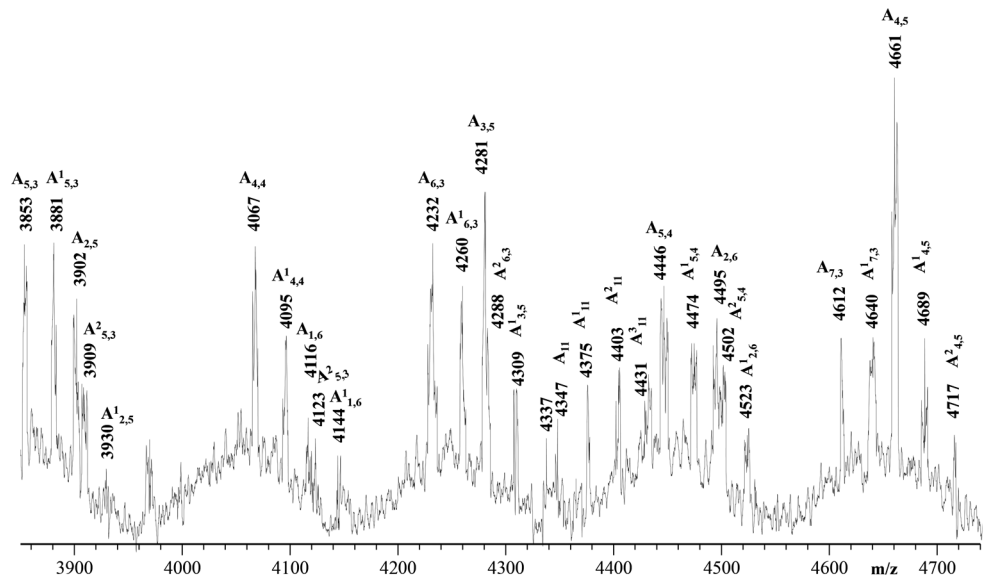

Fig. 5 MALDI-TOF mass spectrum (negative-ion mode) of HA-FA-Pg.

10. Moreover, the shoulder shown by the signal attributed to the anomeric C-a carbon atom of **HA** was interpreted in terms of interaction with the ferulate residue.

Finally, the coupling between the two macromolecular synthons by CuAAC reaction was performed as depicted in Scheme 4.

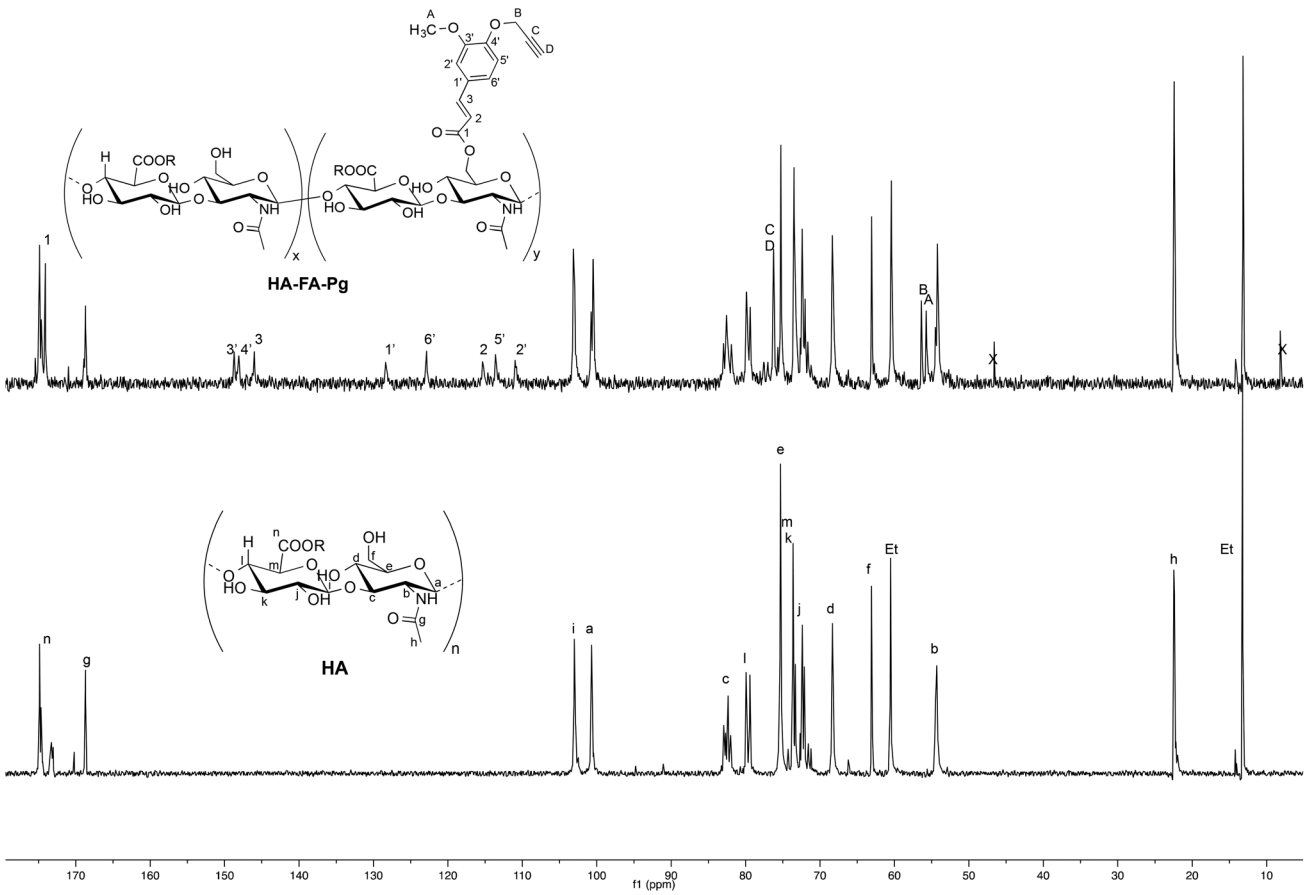

Fig. 6 ^{13}C NMR spectrum (D_2O) of **HA-FA-Pg** compared with that of starting low weight **HA** (D_2O). In the spectrum of **HA**, Et labels indicate the signals of ethyl groups of the monomeric units showing R = C_2H_5.

The use of $CuSO_4$/sodium ascorbate allowed the catalytic system to be generated *in situ* and **TCPB** to be effectively generated under very mild conditions. In order to evaluate the reproducibility of the properties of the **TCPB** material, the coupling reaction was repeated several times by using the same amounts of the two macromolecular synthons (*i.e.* 50 mg of poly-6-ANEGA-CMO-**BF3k-GT** or poly-6-ANEGA-CMO-**BF3k-GO** and 50 mg of **HA-FA-Pg** showing a grafting degree of about 20% corresponding to four propargyl groups per **HA** macromolecule). Because of the large excess of azido groups with respect to the propargyl groups we assumed the almost complete reaction of the latter and the presence in the **TCPB** material of a considerable number of azide moieties to be used for further functionalization by click chemistry. From a structural point of view, the reaction of the randomly alkyne modified hyaluronic acid (bearing at least about 4 clickable units) was assumed to occur with several brush ends, really coating the cylindrical brush-like macromolecules. Thus, the **TCPB** material represents a third-generation polybenzofulvene molecular brush possessing the architecture of a hyaluronan-coated cylindrical brush.

Characterization of the tri-component polymer brush

The **TCPB** material was obtained as a light brown glassy solid by precipitation with acetone from a solution of the copolymer in ethanol–water (2 : 1) and showed an appreciable solubility in water. In fact, when 5 mg of this material were added to 0.5 mL of water, we observed the formation of a transparent gel, which was disrupted by sonication (4 cycles of 15 min at room temperature). The DLS analysis of the water dispersions showed the presence of objects showing colloidal size (DLS data are summarized in Table 2) but, as expected, a great size distribution value was observed because of self-aggregation phenomena.

The ^{13}C NMR spectrum of the **TCPB** material (Fig. 7) was dominated by the signals attributed to NEG side chains and to the low molecular weight **HA** ribbons, whereas the ones belonging to the aromatic carbon atoms of both the polybenzofulvene and ferulate components were lost in the baseline modulations because of line broadening due to the reduced

Table 2 Mean diameter (*Z*-average), polydispersity index (PDI) and zeta potential values of **TCPB** dispersions in ultrapure water

TCPB sample	Z_a (nm)	PDI	Z_p (mV)
TCPB-1	266	0.39	−33.9 ± 7.52
TCPB-2	207	0.35	−32.4 ± 5.56
TCPB-3	209	0.19	−35.3 ± 6.6

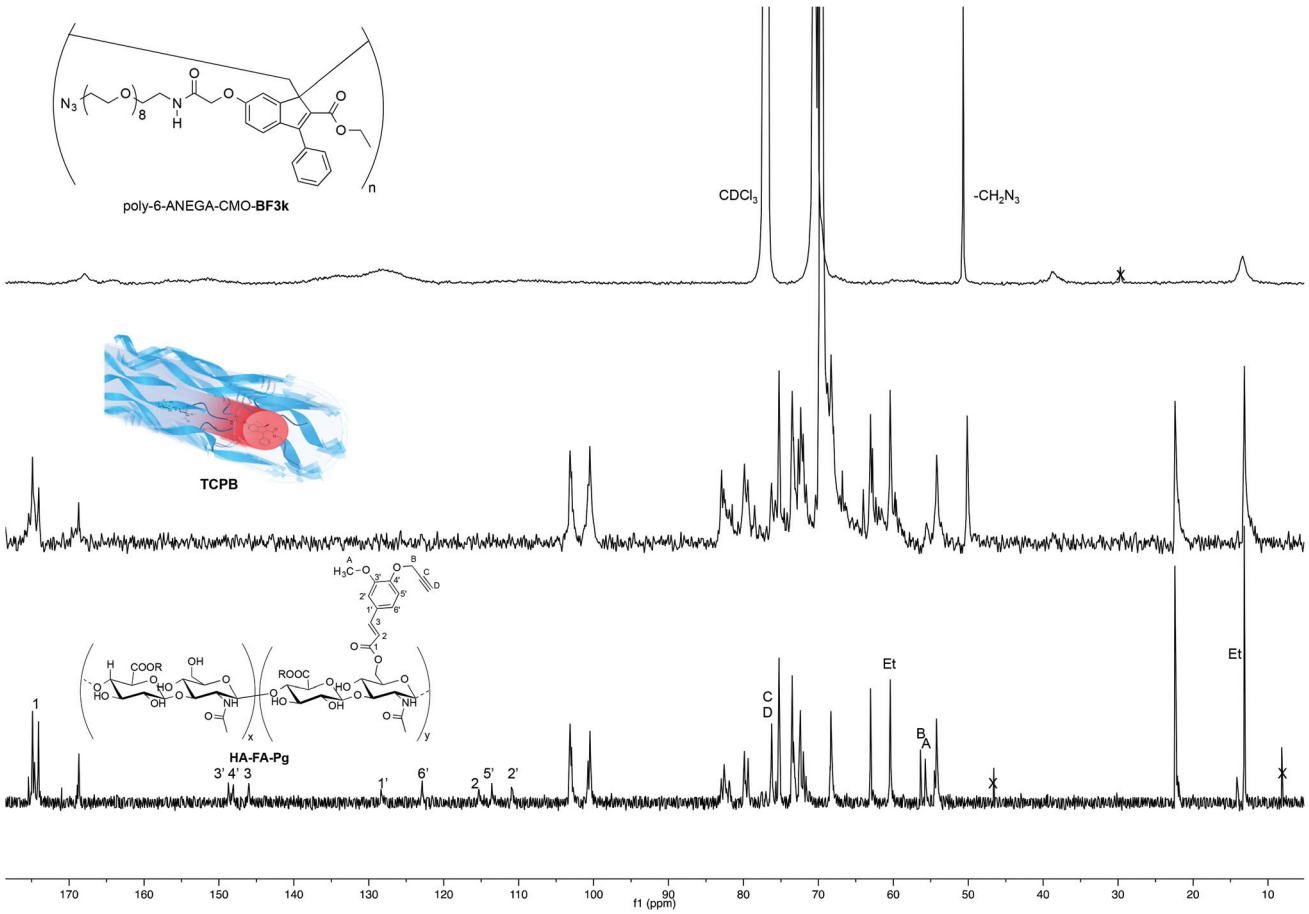

Fig. 7 ^{13}C NMR spectrum (D_2O) of **TCPB** compared with those of polybenzofulvene synthon poly-6-ANEGA-CMO-**BF3k-GT** ($CDCl_3$) and hyaluronan synthon **HA-FA-Pg** (D_2O). In the spectrum of **HA-FA-Pg**, Et labels indicate the signals of ethyl groups of the monomeric units showing R = C_2H_5.

mobility. However, the persistence of a signal at about 56 ppm (attributed to the ferulate methoxy carbon atom, C–A) and the shifting of the ones at about 57 ppm (attributed to the ferulate propargyl carbon C–B) and at about 67 ppm (attributed to the ferulate propargyl carbons C–D and C–C) confirmed the occurrence of the CuAAC coupling reaction between the two macromolecular synthons, which are covalently bound to each other in the **TCPB** material.

Finally, the absorption/emission features (see the ESI†) of the polybenzofulvene backbone of **TCPB** are compatible with its detection in a fluorescence microscopy apparatus with standard filters.[17,21] Thus, the fate and the interactions of **TCPB** could be investigated by fluorescence microscopy.

Preparation and characterization of TCPB nanoparticles

The tri-component polymer brush **TCPB** shows peculiar structural characteristics that make it significant among smart copolymers for drug delivery. Some of these features were already reported for other polybenzofulvene molecular brushes, regarding their ability to complex high molecular weight bioactive molecules, such as immunoglobulin G (IgG),[22] in which the protein–polymer interaction was assumed to occur by non-specific adsorption onto the surface of the hydrogel particles. Moreover, in another recent paper, PBFMBs bearing synthetic dynamic receptors were used to deliver doxorubicin to cancer cells.[21] Actually, the smart features of PBFMBs are closely related to the structure and composition of the resulting material; thus, variations of these characteristics should modify its self-assembling properties, loading capacity and targeting properties. In **TCPB**, for example, the presence of side-chain arms terminated with low molecular weight hyaluronic acid (**HA**) macromolecules conferred to the resulting nanoaggregates a potential CD44 receptor mediated targetability by a receptor mediated uptake in CD44 positive cancer cells. Therefore, **TCPB** nanocarriers were prepared from **TCPB**-3, the material with a lower polydispersity among those synthesized (see Table 2). The ability of **TCPB** to form supramolecular carriers spontaneously, was investigated by means of dynamic light scattering analysis and zeta potential measurements (see Table 3).

Interestingly, the results showed that the **TCPB** nanoparticle sample was formed by a heterogeneous population showing a mean diameter lower than that observed in the nanoaggregates obtained by sonication of the **TCPB**-3 sample in water.

Table 3 DLS results of **TCPB** measured in double distilled water at 25 °C

Sample	*N* distribution (nm)	PDI	Z_p (mV)
TCPB-nanoparticles	123.5	0.19	−30.4 ± 3.8

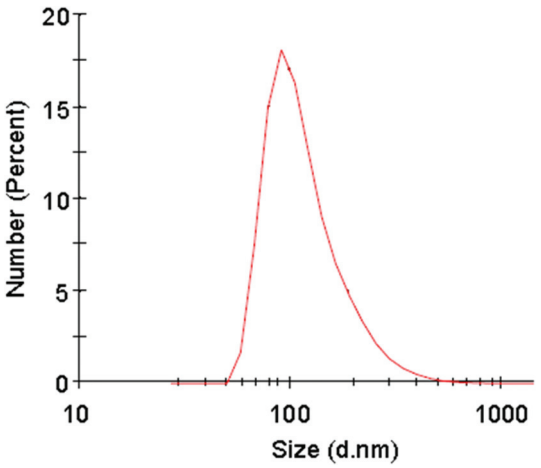

Fig. 8 DLS size distribution histograms of **TCPB** nanoparticle dispersions in ultrapure water.

Thus, the dimensions of **TCPB** nanosystems can be modulated by using different solvent systems. DLS size distribution histograms of **TCPB** nanoparticles are shown in Fig. 8.

Biocompatibility of TCPB nanoparticles

The potential biocompatibility of **TCPB** nanoparticles here prepared was assessed by evaluating their potential cytotoxicity on three different cell lines, namely HCT116 (human colon adenocarcinoma cell lines), MCF-7 (human breast cancer cell lines), and 16HBE (human bronchial epidermal cell lines) after incubation for 24 and 48 h. HCT116 and MCF-7 are two human cancer cell lines with high expression of the CD44 receptor,[4,27] on the contrary 16HBE is a human normal cell used as a CD44-negative cell line. Several concentrations of **TCPB** nanoaggregates were tested on the three cell lines at 24 and 48 h of incubation. Fig. 9 shows that, for both incubation times, 24 h (a) and 48 h (b), nanosystems were clearly cytocompatible in the whole concentration range tested, as the cell viability was always comparable to the control. These data suggest that **TCPB** nanoparticles do not exhibit any selective cytotoxicity, independently by cell line type, pointing out that the **TCPB** nanosystem may be potentially useful as a nanocarrier for the specific delivery of antineoplastic molecules to CD44-overexpressing cancer cells.

Conclusions

On the basis of the pivotal role played by the pericellular **HA** coat in cell adhesion and the largely recognized overexpression of the CD44 receptor in tumor tissues, the family of the polybenzofulvene molecular brushes was enriched by the tricomponent molecular brush **TCPB** bearing hyaluronic acid ribbons. This biomimetic material was designed by functionalizing the polybenzofulvene backbone with nona(ethylene glycol) arms terminated with low molecular weight hyaluronic acid macromolecules. **TCPB** was easily synthesized by means of a convergent approach involving three different steps: the preparation of the polybenzofulvene backbone bearing nona (ethylene glycol) side chains terminated with clickable azido groups, the functionalization of low molecular weight hyaluro-

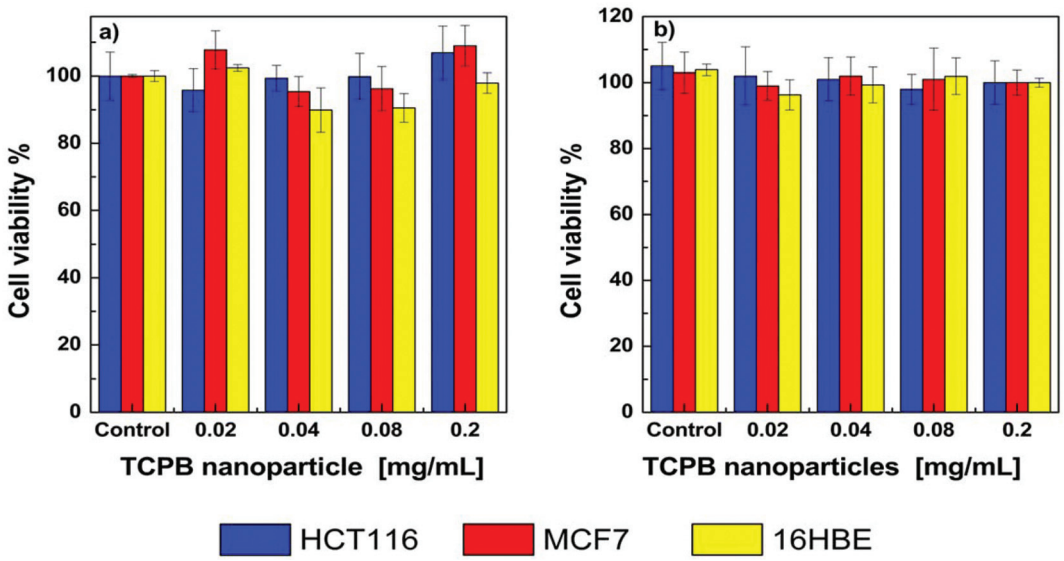

Fig. 9 Cell viability % (MTS assay) of **TCPB** nanoparticles on 16HBE (yellow), MCF-7 (red) and HCT116 (blue) cell lines after 24 h (a) and 48 h (b) of incubation.

nic acid macromolecules with ferulic acid bearing clickable propargyl groups, and the coupling between the two macromolecular synthons by copper(I)-catalyzed azide–alkyne 1,3-dipolar cycloaddition. The **TCPB** material was found to generate colloidal water dispersions containing nanoaggregates in the form of nanoparticles showing a dimension around 120 nm that were devoid of cytotoxicity when tested on three different cell lines with different expression levels of CD44. The tri-component biomimetic architecture together with the interesting preliminary properties of self-organization and the absence of cytotoxicity push **TCPB** toward biomedical applications such as in nanocarriers for drug delivery or materials for tissue engineering.

Conflict of Interest

The authors declare no competing financial interest.

Acknowledgements

Thanks are due to Italian MIUR (Ministero dell'Istruzione, dell'Università e della Ricerca) for financial support.

References

1 M. Cohen, D. Joester, B. Geiger and L. Addadi, Spatial and temporal sequence of events in cell adhesion: from molecular recognition to focal adhesion assembly, *ChemBioChem*, 2004, **5**, 1393–1399.
2 F. Dosio, S. Arpicco, B. Stella and E. Fattal, Hyaluronic acid for anticancer drug and nucleic acid delivery, *Adv. Drug Delivery Rev.*, 2016, **97**, 204–236.
3 Y. Zhong, K. Goltsche, L. Cheng, F. Xie, F. Meng, C. Deng, Z. Zhong and Z. Haag, Hyaluronic acid-shelled acid-activatable paclitaxel prodrug micelles effectively target and treat CD44-overexpressing human breast tumor xenografts in vivo, *Biomaterials*, 2016, **84**, 250–261.
4 V. Orian-Rousseau, CD44, a therapeutic target for metastasising tumours, *Eur. J. Cancer*, 2010, **46**, 1271–1277.
5 R. Langer, New methods of drug delivery, *Science*, 1990, **249**, 1527–1533.
6 R. Langer, Drug delivery and targeting, *Nature*, 1998, **392**, 5–10.
7 M. Licciardi, G. Pitarresi, G. Cavallaro and G. Giammona, Nanoaggregates based on new poly-hydroxyethyl-aspartamide copolymers for oral insulin absorption, *Mol. Pharm.*, 2013, **10**, 1644–1654.
8 M. Licciardi, G. Montana, M. L. Bondì, A. Bonura, C. Scialabba, M. Melis, C. Fiorica, G. Giammona and P. Colombo, An allergen-polymeric nanoaggregate as a new tool for allergy vaccination, *Int. J. Pharm.*, 2014, **465**, 275–283.
9 G. Cavallaro, M. Licciardi, S. Salmaso, P. Caliceti and G. Giammona, Folate mediated targeting of polymeric conjugates of gemcitabine, *Int. J. Pharm.*, 2006, **307**, 258–269.
10 A. Cappelli, G. Pericot Mohr, M. Anzini, S. Vomero, A. Donati, M. Casolaro, R. Mendichi, G. Giorgi and F. Makovec, Synthesis and characterization of a new benzofulvene polymer showing a thermoreversible polymerization behavior, *J. Org. Chem.*, 2003, **68**, 9473–9476.
11 A. Cappelli, M. Anzini, S. Vomero, A. Donati, L. Zetta, R. Mendichi, M. Casolaro, P. Lupetti, P. Salvatici and G. Giorgi, New π-stacked benzofulvene polymer showing thermoreversible polymerization: studies in macromolecular and aggregate structures and polymerization mechanism, *J. Polym. Sci., Part A: Polym. Chem.*, 2005, **43**, 3289–3304.
12 A. Cappelli, G. Pericot Mohr, G. Giuliani, S. Galeazzi, M. Anzini, L. Mennuni, F. Ferrari, F. Makovec, E. M. Kleinrath, T. Langer, M. Valoti, G. Giorgi and S. Vomero, Further studies on imidazo[4,5-*b*]pyridine AT_1 angiotensin II receptor antagonists. Effects of the transformation of the 4-phenylquinoline backbone into 4-phenylisoquinolinone or 1-phenylindene scaffolds, *J. Med. Chem.*, 2006, **49**, 6451–6464.
13 A. Cappelli, S. Galeazzi, G. Giuliani, M. Anzini, A. Donati, L. Zetta, R. Mendichi, M. Aggravi, G. Giorgi, E. Paccagnini and S. Vomero, Structural manipulation of benzofulvene derivatives showing spontaneous thermoreversible polymerization. Role of the substituents in the modulation of polymer properties, *Macromolecules*, 2007, **40**, 3005–3014.
14 A. Cappelli, S. Galeazzi, G. Giuliani, M. Anzini, M. Aggravi, A. Donati, L. Zetta, A. C. Boccia, R. Mendichi, G. Giorgi, E. Paccagnini and S. Vomero, Anionic polymerization of a benzofulvene monomer leading to a thermoreversible π-stacked polymer. Studies in macromolecular and aggregate structure, *Macromolecules*, 2008, **41**, 2324–2334.
15 A. Cappelli, S. Galeazzi, G. Giuliani, M. Anzini, M. Grassi, R. Lapasin, G. Grassi, R. Farra, B. Dapas, M. Aggravi, A. Donati, L. Zetta, A. C. Boccia, F. Bertini, F. Samperi and S. Vomero, Synthesis and spontaneous polymerization of oligo(ethylene glycol)-conjugated benzofulvene macromonomers. A polymer brush forming a physical hydrogel, *Macromolecules*, 2009, **42**, 2368–2378.
16 A. Cappelli, M. Paolino, P. Anzini, G. Giuliani, S. Valenti, M. Aggravi, A. Donati, R. Mendichi, L. Zetta, A. C. Boccia, F. Bertini, F. Samperi, S. Battiato, E. Paccagnini and S. Vomero, Structure–property relationships in densely grafted π-stacked polymers, *J. Polym. Sci., Part A: Polym. Chem.*, 2010, **48**, 2446–2461.
17 A. Cappelli, M. Paolino, G. Grisci, G. Giuliani, A. Donati, R. Mendichi, A. C. Boccia, F. Samperi, S. Battiato, E. Paccagnini, E. Giacomello, V. Sorrentino, M. Licciardi, G. Giammona and S. Vomero, A click chemistry-based "grafting through" approach to the synthesis of a biorelevant polymer brush, *Polym. Chem.*, 2011, **2**, 2518–2527.
18 A. Cappelli, M. Paolino, G. Grisci, G. Giuliani, A. Donati, R. Mendichi, A. C. Boccia, C. Botta, W. Mróz, F. Samperi,

A. Scamporrino, G. Giorgi and S. Vomero, Synthesis and characterization of charge-transporting π-stacked polybenzofulvene derivatives, *J. Mater. Chem.*, 2012, **22**, 9611–9623.

19 A. Cappelli, G. Grisci, M. Paolino, F. Castriconi, G. Giuliani, A. Donati, S. Lamponi, R. Mendichi, A. C. Boccia, F. Samperi, S. Battiato, E. Paccagnini, M. Gentile, M. Licciardi, G. Giammona and S. Vomero, Combining spontaneous polymerization and click chemistry for the synthesis of polymer brushes: A "grafting onto" approach, *Chem. – Eur. J.*, 2013, **19**, 9710–9721.

20 A. Cappelli, M. Paolino, G. Grisci, G. Giuliani, A. Donati, A. C. Boccia, F. Samperi, R. Mendichi and S. Vomero, Reversible polymerization techniques leading to π-stacked polymers, in *π-Stacked Polymers and Molecules*, ed. T. Nakano, Springer, Japan, Osaka, 2014, pp. 51–149.

21 A. Cappelli, G. Grisci, M. Paolino, V. Razzano, G. Giuliani, A. Donati, C. Bonechi, R. Mendichi, A. C. Boccia, M. Licciardi, C. Scialabba, G. Giammona and S. Vomero, Polybenzofulvene derivatives bearing dynamic binding sites as potential anticancer drug delivery systems, *J. Mater. Chem. B*, 2015, **3**, 361–374.

22 M. Licciardi, M. Grassi, M. Di Stefano, L. Feruglio, G. Giuliani, S. Valenti, A. Cappelli and G. Giammona, PEG-benzofulvene copolymer hydrogels for antibody delivery, *Int. J. Pharm.*, 2010, **390**, 183–190.

23 M. Licciardi, G. Amato, A. Cappelli, M. Paolino, G. Giuliani, B. Belmonte, C. Guarnotta, G. Pitarresi and G. Giammona, Evaluation of thermoresponsive properties and biocompatibility of polybenzofulvene aggregates for leuprolide delivery, *Int. J. Pharm.*, 2012, **438**, 279–286.

24 R. Mendichi and A. Giacometti Schieroni, Use of a multi-detector size exclusion chromatography system for the characterization of complex polymers, in *Current Trends in Polymer Science*, ed. S. G. Pandalai, Trans-World Research Network, Trivandrum, India, 2001, vol. 6, pp. 17–32.

25 P. J. Wyatt, Light scattering and the absolute characterization of macromolecules, *Anal. Chim. Acta*, 1993, **272**, 1–40.

26 A. Donati, A. Magnani, C. Bonechi, R. Barbucci and C. Rossi, Solution structure of hyaluronic acid oligomers by experimental and theoretical NMR, and molecular dynamics simulation, *Biopolymers*, 2001, **59**, 434–445.

27 H. Lee, K. Lee and T. G. Park, Hyaluronic acid-paclitaxel conjugate micelles: synthesis, characterization, and anti-tumor activity, *Bioconjugate Chem.*, 2008, **19**, 1319–1325.

